

Road Surface Condition Inspection Using a Laser Scanner Mounted on an Autonomous Driving Car

Kenta Urano
Graduate School of Engineering
Nagoya University
 Aichi, Japan
 vrano@ucl.nuee.nagoya-u.ac.jp

Kei Hiroi
Graduate School of Engineering
Nagoya University
 Aichi, Japan

Shinpei Kato
Graduate School of
Information Science and Technology
University of Tokyo
 Tokyo, Japan

Nozomi Komagata
NICHIREKI CO., LTD.
 Tokyo, Japan

Nobuo Kawaguchi
Institutes of Innovation for Future Society
Nagoya University
 Aichi, Japan

Abstract—Inspection and repair of road infrastructures are important for safety. While highways and motorways are periodically inspected with specialized vehicles, the roads which are maintained by local governments are not inspected because of lack of budget and workforce. In the future, however, a large number of autonomous driving cars will run everywhere. They are equipped with laser scanners to recognize the surroundings. If we utilize these sensors to inspect the road surface condition automatically, the cost of inspection will be reduced dramatically. In this paper, we extract transverse profiles of a road using point clouds which are recorded by a laser scanner mounted on an autonomous driving car. Point clouds are converted to the same format of special vehicle. We compared the data recorded by a specialized vehicle and a car with a laser scanner in Ichinomiya, Aichi prefecture, Japan and found that proposed method can be used as a preliminary survey to find where needs the detailed inspection.

Index Terms—road surface condition, laser scanner, point cloud

I. INTRODUCTION

The maintenance of the aging infrastructures is one of the huge problems related to an insufficient workforce due to a declining birthrate and aging population in Japan. As for road infrastructures, attention has been placed on the ceiling-breakdown accident which occurred in the Sasago tunnel, Japan in 2012, reported that one of the problems were inconsistent maintenance. According to the proposal regarding the full-scale implementation of measures against aging roads by Ministry of Land, Infrastructure, Transport and Tourism (MLITT), Japan, some of the problems preventing from the continuous road infrastructure inspection are: the difficulty of keeping maintenance cycle due to insufficient budget and workforce; and the unplanned management caused by the inconsistent recording and storing of inspection results. Road surface condition inspections using a specialized vehicle (as shown in Fig. 1) require a huge cost even for short

This work was supported by JSPS KAKENHI Grant Number JP17H01762 and by JST-Mirai Program Grant Number JPMJMI17B1.



Fig. 1: Specialized vehicle for inspection.¹



Fig. 2: Example of a road with surface distortion.

distances. Also, because there is only a limited number of specialized vehicles, it is difficult to conduct continuous and comprehensive inspections in a wide area.

Meanwhile, with the development of autonomous driving technology, autonomous driving cars will run everywhere carrying people and cargoes in the future. Autonomous driving cars are equipped with many sensors such as laser scanners, millimeter-wave radars, RGB cameras, etc. to recognize the surroundings, and these cars also carry out self-localization and obstacle detection. If we can inspect the condition of the road and detect defects such as surface distortion and cracks using these sensors, inspection can be done automatically by autonomous driving cars and the cost of inspection will be dramatically reduced .

In this paper, we extract transverse profiles and ruts of the road using a point cloud acquired by a car equipped with a laser scanner and compare them with the data taken by a specialized vehicle. A rut is a kind of road surface distortion as shown in Fig. 2. Rut depth is used as a factor of the Maintenance Control Index (MCI), which is used to evaluate the necessity of maintenance of the road, developed by MLITT. Following steps are used to compare the point cloud collected by the car equipped with the laser scanner with the data collected by a specialized vehicle.

¹https://www.nichireki.co.jp/product/consult/consult_list05/consult05_01.html

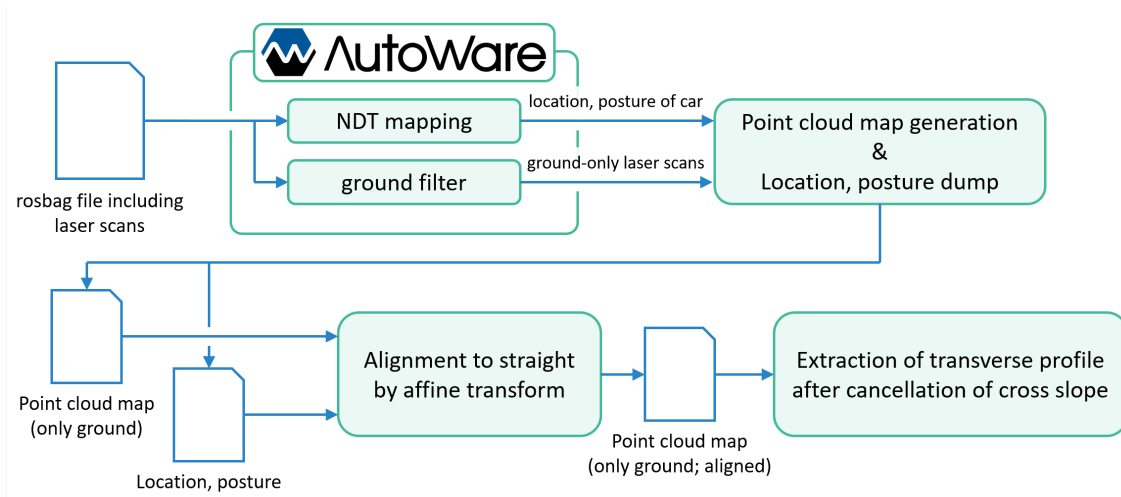


Fig. 3: Data processing flow of proposed method.

(1) A point cloud map without buildings is created from the point cloud. (2) The map is aligned straight using affine transform to remove curvature. (3) Transverse profile data which is the same format as the specialized vehicle is generated using rectangular cells. In addition, we compare the transverse profiles extracted from the point cloud with the data taken by the specialized vehicle and discuss the possibility of the road surface condition inspection using laser scanners.

In Section 2, related work is introduced. The procedure of generation of transverse profile data is explained in detail in Section 3. Comparison of the transverse profiles is stated in Section 4, followed by conclusions in Section 5.

II. RELATED WORK

In the road surface condition inspection, there are various methods[1] such as image-based and acceleration-based, corresponding to the types of road surface defects. For example, there are many image-based methods for detecting cracks. CrackTree[2] aims to detect cracks with higher accuracy by removing the obstructive shadows on the road. The method proposed by Gavil 'a et al.[3] uses SVM to identify the type of road surface (such as the color of asphalt) and changes the parameters of crack detection adaptively for higher accuracy.

Laser scanners can be used to detect cracks and to recognize the crack depth. Tsai et al.[4] conducts crack detection in a low-light environment (nighttime) and argues that a laser scanner is useful for the detection which is not affected by shadows on the road and time of day. Ouyang and Xu[5] use a laser projector and a 3D camera to measure the crack depth. Vehicles used for these methods usually have cameras and laser scanners directed to the road and can acquire detailed information. Such vehicle, however, are custom-built and not able to monitor multiple lanes simultaneously.

Other studies focus on searching for potholes, which results from the detachment of pavement, and evaluating the flatness of the road using accelerometer. Chen et al.[6] calculate the

index related to flatness using an accelerometer. Eriksson et al.[7] collected data by equipping an accelerometer into a taxi in Boston, the USA for pothole detection. Because rapid acceleration change is recorded at every bump, they excluded bridge joints, manholes etc. from the places estimated to have abnormal road surface. Mednis et al.[8] used the accelerometer of Android devices as the measuring equipment. Acceleration based method needs complicated algorithms for accurate detection of small defects because the information recorded by the onboard accelerometer is affected by the suspensions or the tires of a car.

For transverse profile recognition, Li et al.[9] proposed a method that uses one laser scanner and two cameras. With careful calibration, detection of road surface distortion, speed bumps, potholes, etc. are carried out. Hui et al.[10], however, states that cover width of a laser scanner should be expanded to acquire transverse profile accurately from the result of their experiment for the measurement errors caused by vehicle wandering.

In this paper, we investigate the possibility of a road surface condition inspection using only a laser scanner attached to the roof of a vehicle. Since this sensor is for recognition of the surroundings and for self-localization, the acquired point cloud includes structures other than the road surface, such as other vehicles, pedestrians, and buildings. Although such structures must be removed, a roof-mounted laser scanner can collect information of multiple lanes at once, compared to the methods which need road-facing sensors. Moreover, in an environment where many autonomous driving cars run, information is collected constantly and that leads to dense inspection with regard to time.

On the other hand, the distance from the laser scanner to the road surface is longer compared to the specialized vehicle. That leads the increase of measurement errors and prevents us from detailed inspection of cracks. Therefore, in this paper, we extract transverse profiles as the road surface condition

obtained from point clouds and compare them with the data from the specialized vehicle.

III. TRANSVERSE PROFILE EXTRACTION FROM POINT CLOUD

Overview of the proposed method is shown in Fig. 3. First, a rosbag file including laser scans is processed by Autoware[11], which is the open source software for autonomous driving. Two kinds of data are obtained using the Normal Distributions Transform (NDT)[12] mapping function of Autoware: (1) the vehicle position/orientation, (2) the ground-only laser scans. By translating the ground-only laser scans based on the vehicle position/orientation, the ground-only point cloud map is generated. Next, to remove the curvature of the road, the ground-only point cloud map is aligned straight using affine transform. Finally, the transverse profile which format is same as that detected by a specialized vehicle after removing the cross slope.

A. Ground-only Point Cloud Map

Generating a ground-only point cloud map depends on two functions provided by Autoware: NDT mapping and ground filter. NDT mapping is basically used for self-localization and generates the position and the orientation of the vehicle. Ground filter separates the points recorded by the laser scanner into ground-only part and non-ground (buildings, pedestrians etc.) part.

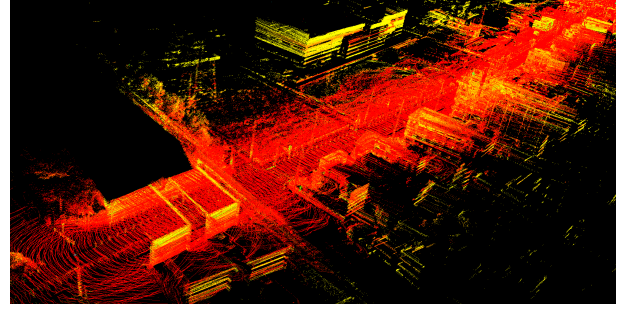
We developed a program which works as a node of the Robot Operating System (ROS) and creates a ground-only point cloud map by translating ground-only part based on vehicle position/orientation. Fig. 4 shows a point cloud map generated by NDT mapping and a ground-only point cloud map. Building-like structures are removed in Fig. 4(b).

B. Alignment of Point Cloud Map by Affine Transform

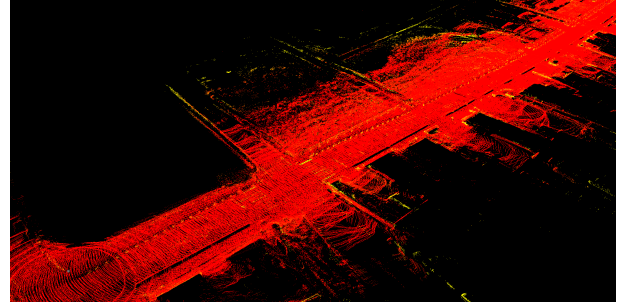
The ground-only point cloud map still includes the points which are other than the road such as parking lots and firms. Moreover, the road in the map is not straight. Therefore, alignment using affine transform based on the vehicle position/orientation is performed to remove non-road points and make the road straight for further processing. In the alignment process, the road is aligned to run along with x-axis.

Before applying the affine transform, some positions are removed from the vehicle position/orientation. When the vehicle pauses at a traffic light, NDT mapping outputs same positions. The positions which satisfy the distance of two consecutive positions is less than 1.5 m are removed.

Then, for the vehicle position at time t , $c_t = (x_{c_t}, y_{c_t})$, the positions 10 m to the left and right, l_t and r_t , perpendicular to the direction towards $c_{t+1} = (x_{c_{t+1}}, y_{c_{t+1}})$ from c_t . These points, $l_t = (x_{l_t}, y_{l_t})$ and $r_t = (x_{r_t}, y_{r_t})$, are defined as (1) and (2). Here, θ_t is defined as (3).



(a) Point cloud map generated by NDT mapping function.



(b) Ground-only point cloud map.

Fig. 4: Generation of a point cloud map from a rosbag file. Buildings are removed in Fig. 4(b).

$$\begin{bmatrix} x_{l_t} \\ y_{l_t} \end{bmatrix} = \begin{bmatrix} x_{c_t} \\ y_{c_t} \end{bmatrix} + 10 \begin{bmatrix} \cos(\theta_t + \frac{\pi}{2}) \\ \sin(\theta_t + \frac{\pi}{2}) \end{bmatrix} \quad (1)$$

$$\begin{bmatrix} x_{r_t} \\ y_{r_t} \end{bmatrix} = \begin{bmatrix} x_{c_t} \\ y_{c_t} \end{bmatrix} + 10 \begin{bmatrix} \cos(\theta_t + \frac{3\pi}{2}) \\ \sin(\theta_t + \frac{3\pi}{2}) \end{bmatrix} \quad (2)$$

$$\theta_t = \arctan \frac{y_{c_{t+1}} - y_{c_t}}{x_{c_{t+1}} - x_{c_t}} \quad (3)$$

Next, for l_t and r_t , the points l'_t , r'_t , which are after the translation by the affine transform, are defined as (4) and (5). Here, d_a is the cumulative travel distance of the vehicle up to the time t , which is defined as (6). However, in the case of $t = 0$, it is set to be the distance from the origin of c_0 .

$$\begin{bmatrix} x_{l'_t} \\ y_{l'_t} \end{bmatrix} = \begin{bmatrix} d_a \\ 10 \end{bmatrix} \quad (4)$$

$$\begin{bmatrix} x_{r'_t} \\ y_{r'_t} \end{bmatrix} = \begin{bmatrix} d_a \\ -10 \end{bmatrix} \quad (5)$$

$$d_a = \sum_{\tau=0}^t \sqrt{(c_{x_\tau} + c_{x_{\tau-1}})^2 + (c_{y_\tau} + c_{y_{\tau-1}})^2} \quad (6)$$

Finally, the points in the rectangle $l_t, r_t, l_{t+1}, r_{t+1}$ are translated to the corresponding points in $l'_t, r'_t, l'_{t+1}, r'_{t+1}$. In the translation, two affine transforms (1) l_t, r_t, l_{t+1} to l'_t, r'_t, l'_{t+1} for the points in l_t, r_t, l_{t+1} ; and (2) r_t, l_{t+1}, r_{t+1} to r'_t, l'_{t+1}, r'_{t+1} for the points in r_t, l_{t+1}, r_{t+1} are used. The points which are not in any triangle are simply ignored. Doing this operation for all vehicle positions, the point cloud map

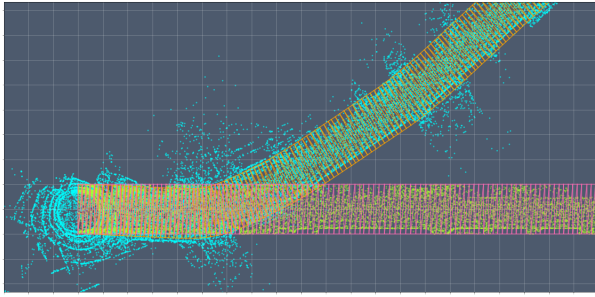


Fig. 5: Alignment of a point cloud map. Cyan dots: original points, green dots: transformed points.

TABLE I: One-way distance of each path.

| Location | Distance (m) | (Latitude, longitude) of endpoints |
|----------|--------------|--|
| A | 460 | (35.26325, 136.7735) and (35.26345, 136.7785) |
| B | 696 | (35.30365, 136.8431) and (35.30333, 136.8508) |

is transformed into a straight line. Fig. 5 shows an example of alignment using affine transformation. In the figure, the points before translation are shown in cyan dots, the points after translation are shown in yellow dots. The triangles for affine transform are shown in orange (before) and pink (after).

The curvature of the road is corrected to straight after affine transform and the points that do not belong to any triangle do not appear.

C. Cancellation of Cross Slope and Generation of Transverse Profile

In the point cloud map aligned straight by affine transform, the x-axis corresponds to the traveling direction on the road and the y-axis corresponds to the transverse direction of the road. For the generation of transverse profiles, the point cloud map is divided every 1 m (for x-axis) x 5 cm (for y-axis) into cells. After that, the average of the z-direction (height) values of points belonging to each cell is calculated to give the height of that cell.

On the other hand, the road surface has the cross slope for water drainage. Since the data from a specialized vehicle is processed to make outer lane markings and center lane marking be at 0 mm height, the same processing is also applied to the transverse profiles calculated from the point cloud map.

IV. COMPARISON WITH SPECIALIZED VEHICLE

A. Data Collection

The data used for the evaluation was acquired at two different locations in Ichinomiya, Aichi prefecture, Japan. The one-way distance of each path is shown in Table I. The views of pavements of actual locations are shown in Fig. 6. In the data collection, a special vehicle of NICHIREKI Co., LTD. and a car with a laser scanner² measured each location. The

²Velodyne VLP-16



(a) Location A.

(b) Location B.

Fig. 6: Views of actual locations.

specialized vehicle took a round trip at each location at about 30 km/h. The car with the laser scanner made two round trips and collected four measurements on one lane (since the laser scanner can measure two lanes simultaneously) at about 20 km/h.

B. Comparison of Transverse Profile

Fig. 7 shows the examples of qualitative results of the transverse profiles extraction. The data used here is from the location B. Each transverse profile shown in the figure is arranged to show two lanes, with one lane at the left and another lane at the right of $x = 0$. The purple line shows the profile recorded by the specialized vehicle and the lines in red, yellow, green, cyan indicate the profiles calculated from the car with the laser scanner. In addition, the blue dotted line corresponds to the average profile of four profiles.

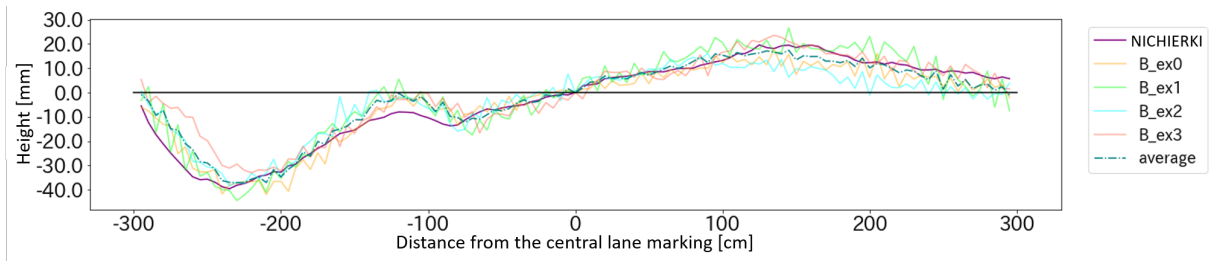
Figs. 7(a) and 7(b) are the examples in which the profiles fit with each other. Figs. 7(c) and 7(d) are the examples in which the profiles do not fit. For Fig. 7(c), the reason of failure is that a curbstone is mistakenly used as the outer lane marking when the cross slope is canceled. For Fig. 7(d), something which remained after the ground filter caused 800 mm height.

Averaging multiple measurements mitigates each measurement's jagging. From this result, using multiple measurements improves the accuracy, even if a single measurement cannot grasp the profile accurately. It means the more autonomous driving cars run, the more accurate result we can expect.

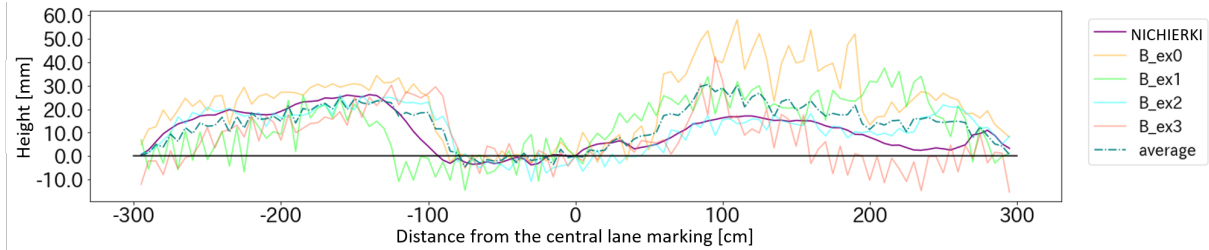
C. Error Distribution

Fig. 7 showed the qualitative results, however, we have to know how deep is a rut. Therefore, we created scatter plots, shown in Fig. 8, for the road surface height obtained by the specialized vehicle on the horizontal axis and the road surface height calculated from the point cloud maps on the vertical axis. If the extraction of the transverse profile is successful, all points in the figures overlap the black lines, which shows $y = x$. On the other hand, the red lines show $y = rx$ with r as the coefficient between the data from the specialized vehicle and the data calculated from the point cloud map. For the calculation of r , we removed the points where the height values are outside the range of $[-200, 200]$ mm as outliers.

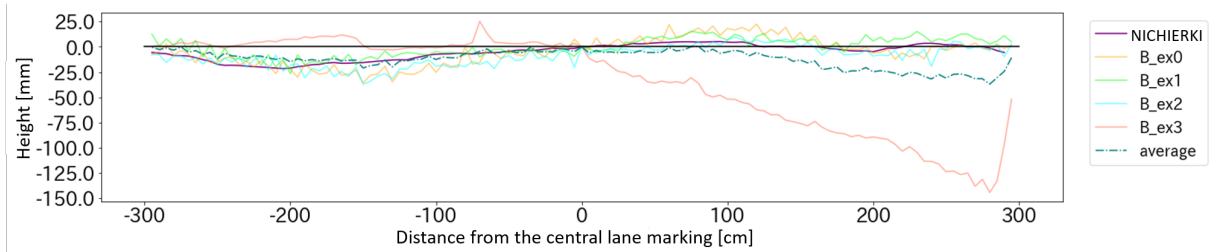
From the figures, in the location A, the maximum depth is at most around 20 mm and correlation is weak. On the other hand, in the location B, the maximum depth is deeper than the location A and correlation is strong. From the result, inspection by the car with the laser scanner can detect deep



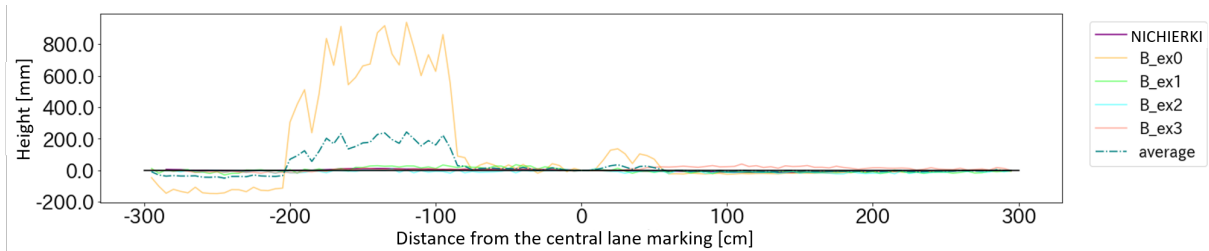
(a) Good example (1): each profile looks alike.



(b) Good example (2): averaging multiple profiles mitigates jagging.



(c) Bad Example: cancellation of cross slope was not successful.



(d) Bad Example: an object on the road was not removed.

Fig. 7: Transverse profile comparison.

rut. Therefore, it can be used to find the locations where needs a detailed inspection for immediate repair.

V. CONCLUSION

In this paper, we extracted the transverse profile of the road from the data collected by a car with a laser scanner mounted on the roof. The data is processed by Autoware, followed by alignment to straight and cancellation of cross slope. Transverse profile, which has the same format as the specialized vehicle, is generated by dividing the data into rectangular cells.

For comparison, a car with a laser scanner and a specialized vehicle acquired the data at two locations in Ichinomiya, Aichi prefecture, Japan. The comparison revealed that the transverse

profile can be obtained from the data of the laser scanner. There were some failures in ground filtering and in cross slope cancellation. On the other hand, taking the average of multiple measurements improved the accuracy. From the comparison, the inspection using the car with the laser scanner can be effective for finding the locations where needs further inspection for immediate repair.

Future tasks for an improved result will be: elimination of outliers; lane recognition for robust cross slope cancellation. Data collection from various locations is also needed. Moreover, continuous data collection is required to monitor a temporal change of the rut depth.

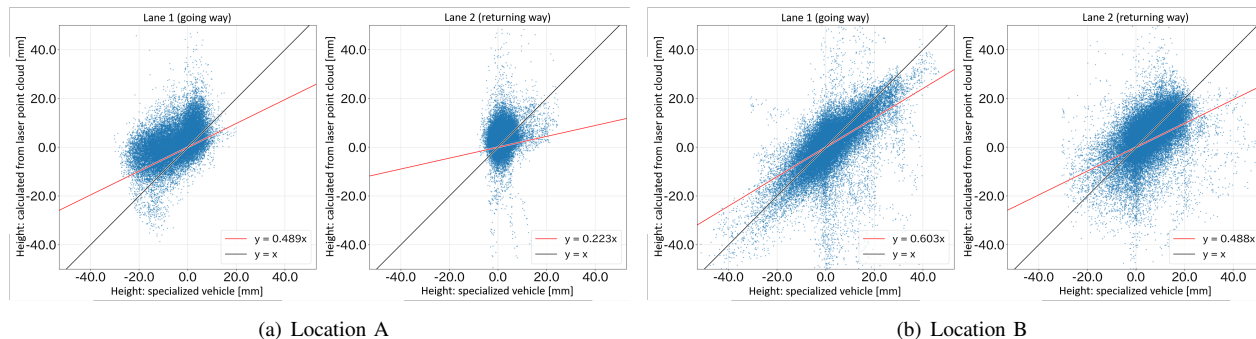


Fig. 8: Correlation of road surface height between specialized vehicle and point cloud.

REFERENCES

- [1] Sylvie Chambon and Jean-Marc Moliard. Automatic Road Pavement Assessment with Image Processing: Review and Comparison. *International Journal of Geophysics*, 2011:1–20, 2011.
- [2] Qin Zou, Yu Cao, Qingquan Li, Qingzhou Mao, and Song Wang. CrackTree: Automatic Crack Detection from Pavement Images. *Pattern Recognition Letters*, 33(3):227–238, 2012.
- [3] Miguel Gavilán, David Balcones, Oscar Marcos, David F. Llorca, Miguel A. Sotelo, Ignacio Parra, Manuel Ocaña, Pedro Aliseda, Pedro Yarza, and Alejandro Amírola. Adaptive Road Crack Detection System by Pavement Classification. *Sensors*, 11(10):9628–9657, 2011.
- [4] Yi-Chang James Tsai and Feng Li. Critical Assessment of Detecting Asphalt Pavement Cracks under Different Lighting and Low Intensity Contrast Conditions using Emerging 3D Laser Technology. *Journal of Transportation Engineering*, 138(5):649–656, 2012.
- [5] W. Ouyang and B. Xu. Pavement Cracking Measurements using 3D Laser-scan Images. *Measurement Science and Technology*, 24(10), 2013.
- [6] Kongyang Chen, Mingming Lu, Xiaopeng Fan, Mingming Wei, and Jinwu Wu. Road Condition Monitoring using On-board Three-axis Accelerometer and GPS Sensor. In *6th International ICST Conference on Communications and Networking in China (CHINACOM)*, pages 1032–1037, 2011.
- [7] Jakob Eriksson, Lewis Girod, Bret Hull, Ryan Newton, Samuel Madden, and Hari Balakrishnan. The Pothole Patrol: Using a Mobile Sensor Network for Road Surface Monitoring. In *6th International Conference on Mobile Systems, Applications, and Services, MobiSys '08*, pages 29–39. ACM, 2008.
- [8] Artis Mednis, Girts Strazdins, Reinholds Zviedris, Georgijs Kanonirs, and Leo Selavo. Real Time Pothole Detection using Android Smartphones with Accelerometers. In *2011 International Conference on Distributed Computing in Sensor Systems and Workshops (DCOSS)*, pages 1–6, 2011.
- [9] Qingguang Li, Ming Yao, Xun Yao, and Bugao Xu. A Real-time 3D Scanning System for Pavement Distortion Inspection. *Measurement Science and Technology*, 21(1), 2010.
- [10] Bing Hui, Yichang (James) Tsai, Mu Guo, and Xiaofang Liu. Critical Assessment of the Impact of Vehicle Wandering on Rut Depth Measurement Accuracy using 13-point Based Lasers. *Measurement*, 123:246–253, 2018.
- [11] Shinpei Kato, Eijiro Takeuchi, Yoshio Ishiguro, Yoshiki Ninomiya, Kazuya Takeda, and Tsuyoshi Hamada. An Open Approach to Autonomous Vehicles. *IEEE Micro*, 35(6):60–68, 2015.
- [12] Peter Biber and Wolfgang Straer. The Normal Distributions Transform: A New Approach to Laser Scan Matching. In *IEEE International Conference on Intelligent Robots and Systems*, volume 3, pages 2743–2748, 11 2003.